

# A novel compatibilizer for the toughening of unsaturated polyester resins

G. RAGOSTA\*, M. BOMBACE, E. MARTUSCELLI, P. MUSTO, P. RUSSO, G. SCARINZI

*National Research Council of Italy, Institute of Research and Technology of Plastic Materials, Via Toiano n. 6, 80072 Arco Felice (Na), Italy*

A block-copolymer of the type A–B–A was synthesized from a commercial polybutadiene rubber (PBD) and an unsaturated polyester (UP) prepolymer. The reaction process was monitored via Fourier transform–infrared spectroscopy. The obtained copolymer was used as compatibilizing agent for UP/PBD blends. Fracture measurements performed on the cured materials demonstrated a substantial enhancement of toughness in the presence of the copolymer. The morphological analysis of the fracture surfaces showed that the presence of the compatibilizing agent produced a strong reduction of the size of the rubber particles, a better interface adhesion and an increase of localized shear yielding in the UP matrix around the rubber particles. © 1999 Kluwer Academic Publishers

## 1. Introduction

Unsaturated polyester (UP) resins represent one of the most important matrices for composite applications [1, 2]. They are particularly useful in sheet moulding compounds (SMC) and bulk moulding compounds (BMC) for manufacturing automotive parts [3, 4]. In common with other thermosets, they are intrinsically brittle. The well-developed technique of rubber toughening has had a very limited success in the case of UP resins. This is because of the reduced solubility of the rubber component in the unreacted resin and the poor chemical reactivity of the rubber toward the polyester functionalities.

To overcome these drawbacks, we have chemically modified a number of commercially available liquid rubbers in order to enhance their reactivity toward the UP end-groups. In particular, in previous works [5, 6], a hydroxyl-terminated polybutadiene rubber and an amino-terminated butadiene acrylonitrile copolymer were transformed into an isocyanate-terminated polybutadiene and in a meleimide-terminated rubber, respectively. Interesting results in terms of toughness and morphology were obtained when these modified rubbers were employed as toughening agents for UP resins.

In the present paper, an alternative approach to toughen unsaturated polyester resins is reported. It consists in the synthesis of a suitable block copolymer of the type A–B–A (polyester–rubber–polyester) and in the use of this copolymer as a compatibilizing agent in UP/rubber blends.

The copolymerization reaction was followed by Fourier transform–infrared spectroscopy (FT–IR) and the same technique was used for the characterization of the cured materials.

The fracture properties were investigated at low and high rate of deformation, using the linear elastic fracture mechanics (LEFM) approach. The fracture data were interpreted in the light of the morphological analysis performed on the fracture surfaces by scanning electron microscopy (SEM).

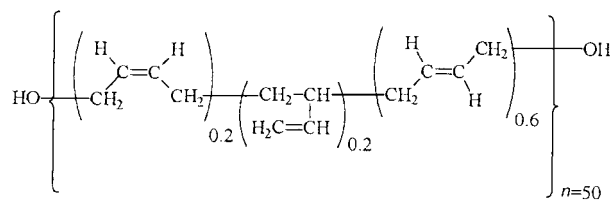
## 2. Experimental procedure

### 2.1. Materials

The resin was an uncured, unsaturated polyester (UP) kindly supplied by Lonza S.p.A. The resin was available either as a solution containing 35% styrene or in the form of the neat prepolymer, without solvent. The polyester prepolymer had  $\bar{M}_n = 1500 \text{ g mol}^{-1}$ .

The acid number, defined as the amount (mg) of KOH used for the titration of 1 g prepolymer, was 33.3. The OH number, obtained by titration of the excess acetic anhydride used to esterify fully the hydroxyl groups, was 40.9. This corresponds to 0.59 mmol COOH groups and 0.73 mmol OH groups per gram of resin. The OH functionality, evaluated from the above titrations, corresponds to 1.1. In the UP formulation, 0.1% by weight of hydroquinone was employed as inhibitor to prevent premature curing. Benzoyl peroxide (BOP) was the radical initiator. The liquid rubber was a hydroxyl-terminated polybutadiene (PBD) produced by ELF ATOCHEM with  $\bar{M}_n = 1600 \text{ g mol}^{-1}$ ,  $\bar{M}_w = 4200 \text{ g mol}^{-1}$ , polydispersity = 2.6 and functionality = 2.1. The toluene diisocyanate (TDI) was a 65/35 wt/wt mixture of 2.4 and 2.6 isomers. The chemical formula of the PBD (I) is shown below.

\* Author to whom all correspondence should be addressed.



(I)

## 2.2. Preparation of the isocyanate terminated polybutadiene (PBDI) rubber

11.58 g PBD were mixed in a glass vessel with 2.8 ml TDI (mole ratio NCO/OH = 2/1) at 60°C under nitrogen with vigorous mechanical stirring for 1 h. Further experimental details are reported elsewhere [5].

## 2.3. Synthesis of the block copolymer (UP-PBD-UP)

27.0 g UP were dissolved in 350 ml CHCl<sub>3</sub> passed over basic alumina. The solution was added to a round-bottomed flask containing the PBDI rubber. After complete dissolution of the rubber, the solution was heated at reflux under a nitrogen atmosphere and magnetic stirring. After 5 h the complete conversion of the isocyanate groups was checked by FT-IR spectroscopy. The product was isolated by solvent evaporation under vacuum.

## 2.4. Preparation of a typical UP/PBD rubber blend

7 g PBD rubber along with 63 g UP were added to a round-bottomed flask. The flask was heated to 60°C under vigorous mechanical stirring for 2 h. The blend was then cooled to 40°C and 0.63 g BPO were added (1% wt/wt with respect to UP), while continuing the stirring. Upon the BPO dissolution (30 min) the flask was cooled to room temperature and the mixture was degassed under vacuum. The mixture was then poured in a glass mould and immersed in a thermostatic water bath for 2 h at 50°C and 10 h at 70°C. The cured blend was finally postcured for 2 h at 100°C. The same procedure was used for the preparation of binary and ternary blends, whose composition is reported in Table I.

## 2.5. Techniques

Transmission infrared spectra were obtained at 4 cm<sup>-1</sup> resolution with a Perkin-Elmer FT-IR spectrometer model System 2000, equipped with a deuterated triglycine sulphate detector (DTGS) and a germanium/KBr beam splitter. The recorded wave number range was 4000–400 cm<sup>-1</sup> and 30–50 spectra were signal-averaged in the conventional manner to reduce the noise. The FT-IR analysis of the UP-PBD-UP copolymer was performed on CHCl<sub>3</sub> solutions. The liquid-cell thickness was chosen so as to keep the absorbance of the region of interest in a range where the Lambert-Beer law is obeyed. The FT-IR spectra of the uncured UP and blends were collected on thin films ob-

TABLE I Composition of the investigated blends

| UP<br>(parts by weight) | PBD<br>(parts by weight) | Copolymer<br>(parts by weight) |
|-------------------------|--------------------------|--------------------------------|
| 100                     | —                        | —                              |
| 96                      | 4                        | —                              |
| 92                      | 8                        | —                              |
| 90                      | 10                       | —                              |
| 85                      | 15                       | —                              |
| 96                      | 4                        | 1                              |
| 92                      | 8                        | 1                              |
| 90                      | 10                       | 1                              |
| 85                      | 15                       | 1                              |
| 96                      | 4                        | 3                              |
| 92                      | 8                        | 3                              |
| 90                      | 10                       | 3                              |
| 85                      | 15                       | 3                              |
| 96                      | 4                        | 5                              |
| 92                      | 8                        | 5                              |
| 90                      | 10                       | 5                              |
| 85                      | 15                       | 5                              |

tained by sandwiching a drop of the reactive mixture between two KBr windows. The cured materials were finely ground and analysed via FT-IR using the KBr pellet technique.

Differential scanning calorimetry (DSC) measurements were carried out on a Mettler TA 3000 instrument. The scanning rate was 20°C min<sup>-1</sup>.

Dynamic-mechanical measurements at 1 Hz were made in the single-cantilever bending mode between -100 and 200°C using a MK III DMTA apparatus from Polymer Laboratories; the scanning rate was 2°C min<sup>-1</sup>.

Three-point bending specimens were used to perform fracture tests at room temperature at low and high strain rates. The low strain-rate measurements were carried out on an Instron apparatus Model 4505 at a crosshead speed of 1 mm min<sup>-1</sup>. The high strain-rate tests were performed on a Charpy instrumented pendulum at room temperature and at an impact speed of 1 m s<sup>-1</sup>. For both tests, samples 60 mm long, 6.0 mm wide and 5.0 mm thick were cut from sheets of the cured resins. Prior to testing, the samples were sharply notched. The fracture data were analysed according to the concepts of linear elastic fracture mechanics (LEFM) [7].

The critical stress intensity factor,  $K_{Ic}$ , was calculated using the following equation

$$K_{Ic} = \sigma Y a^{1/2} \quad (1)$$

where  $\sigma$  is the nominal stress at the onset of crack propagation,  $a$  is the initial crack length, and  $Y$  is a calibration factor depending upon the specimen geometry. For three-point bending specimen,  $Y$  is given by Brown and Srawley [8]. For the determination of the critical strain energy release rate,  $G_c$  the following equation was used

$$G_c = \frac{U}{BW\phi} \quad (2)$$

where  $U$  is the fracture energy,  $B$  and  $W$  are the thickness and the width of the specimen, respectively, and  $\phi$

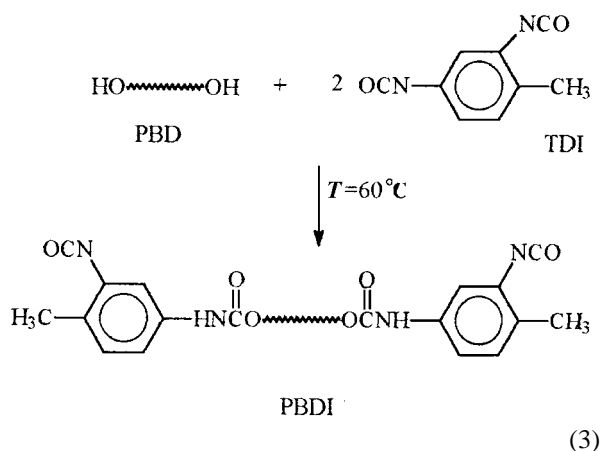
is a calibration factor which depends on the length of the notch and the size of the sample. Values of  $\phi$  were taken from Plati and Williams [9].

Fracture surfaces were coated with a thin layer of a gold-palladium alloy and then examined by scanning electron microscopy (SEM).

### 3. Results and discussion

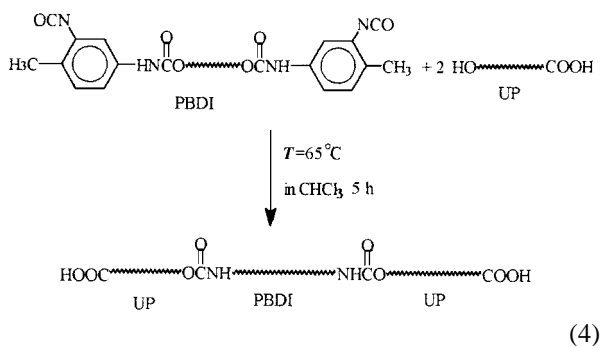
#### 3.1. Synthesis and characterization of the UP-PBD-UP copolymer

The preparation of the copolymer to be used as compatibilizing agent was carried out in two steps. In the first step, the hydroxyl end-groups of the PBD rubber were transformed into isocyanate groups (PBDI) by reaction with toluene diisocyanate (TDI), as follows



FT-IR spectroscopic analysis of the reaction product, whose details are reported elsewhere [5], demonstrated that the final conversion of the hydroxyl groups into isocyanate functionalities was essentially complete ( $\alpha \geq 95\%$ ).

In the second step, the PBDI rubber was allowed to react with a stoichiometric amount of the polyester prepolymer leading to the formation of a three-block copolymer of the UP-PBD-UP type (Reaction 2)



Obviously, the reaction product reported in the above formula is the largely prevailing one. Other structures are likely to form, however, although to a limited extent, due to the presence of a small fraction of polyester chains having both OH or COOH end-groups.

The kinetic of this process was monitored by FT-IR spectroscopy following the intensity decrease with time of the  $\nu_{\text{NCO}}$  absorption at  $2275 \text{ cm}^{-1}$ . In Fig. 1, the FT-IR spectra collected at different times, in the

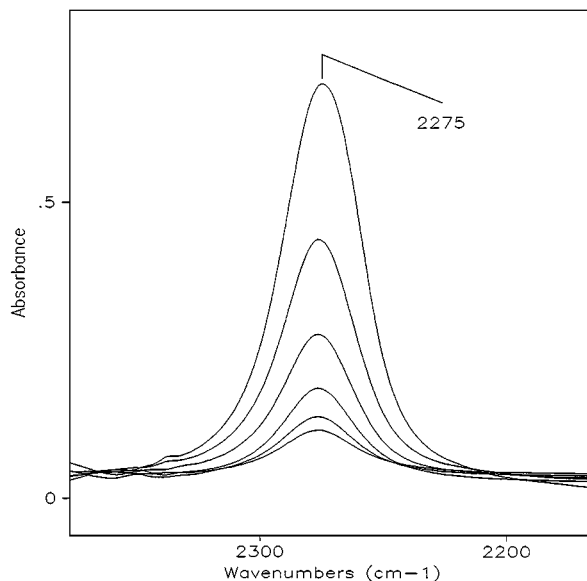


Figure 1 Transmission FT-IR spectra in the frequency range  $2400\text{--}2150 \text{ cm}^{-1}$  of the PBDI/UP solution in  $\text{CHCl}_3$  at different reaction times. Cell thickness 0.2 mm.

$2180\text{--}2370 \text{ cm}^{-1}$  range, are reported. From the above spectra data, it was possible to quantify the isocyanate group conversion  $\alpha$ , using the following equations

$$\alpha(t) = \frac{[\text{NCO}]_0 - [\text{NCO}]_t}{[\text{NCO}]_0} = 1 - \frac{[\text{NCO}]_t}{[\text{NCO}]_0} \quad (5)$$

and, on the basis of the Lambert and Beer law

$$A = \epsilon l [\text{NCO}] \quad (6)$$

$$\alpha(t) = \left( 1 - \frac{A_t}{A_0} \right) \quad (7)$$

where the symbols have the usual meaning and the subscripts 0 and  $t$  refer to the reaction times 0 and  $t$ , respectively. In Fig. 2, the conversion data are reported as a function of time. Curve A refers to a non-catalysed system, and curve B to a catalysed system containing 0.4 wt % dibutyl tin dilaurate (DBTDL). In the case

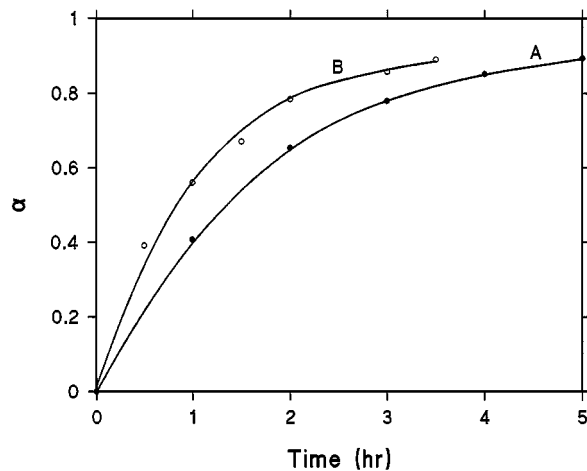


Figure 2 The relative conversion,  $\alpha$ , of the  $\text{--NCO}$  group as a function of the reaction time in the system PBDI/UP in  $\text{CHCl}_3$  at  $60^\circ\text{C}$ ; uncatalysed reaction (curve A), catalysed reaction (curve B).

of the uncatalysed reaction, full conversion is reached after 5 h, while for the catalysed reaction the process is completed after 3 h. The isocyanate conversion kinetic can be conveniently described by the equation

$$\frac{d\alpha}{dt} = Kf(\alpha) \quad (8)$$

where  $K$  is an overall kinetic constant and its dependence on temperature follows the Arrhenius law

$$K = A \exp(-E_a/RT) \quad (9)$$

$f(\alpha)$  is a conversion function and of the form

$$f(\alpha) = (1 - \alpha)^n \quad (10)$$

where  $n$  is the pseudo reaction order.

Integrating Equation 8 for  $n = 0, 1$  and  $2$ , the following expressions are obtained

$$\alpha = Kt \quad n = 0 \quad (11)$$

$$-\ln(1 - \alpha) = Kt \quad n = 1 \quad (12)$$

$$\frac{\alpha}{1 - \alpha} = Kt \quad n = 2 \quad (13)$$

A good linear correlation of the kinetic data is obtained only when Equation 12 is used. The parameter  $-\ln(1 - \alpha)$  versus  $t$  is reported in Fig. 3.

In agreement with Equation 12, a linear trend is obtained for both the catalysed and uncatalysed reactions (curves B and A, respectively). In both cases the reaction between the UP and PBDI follows a pseudo first-order kinetic. The kinetic constant,  $K$ , can be calculated from the slopes of the curves. A value of  $0.452 \text{ h}^{-1}$  is obtained for the uncatalysed reaction, while the catalysed reaction shows a  $K$  value of  $0.612 \text{ h}^{-1}$ . The presence of the catalyst increases the kinetic constant by 1.35 times.

A DSC analysis has been also performed on the obtained copolymer. Fig. 4 shows thermograms relative to the PBD (curve A), uncured UP resin (curve B) and the

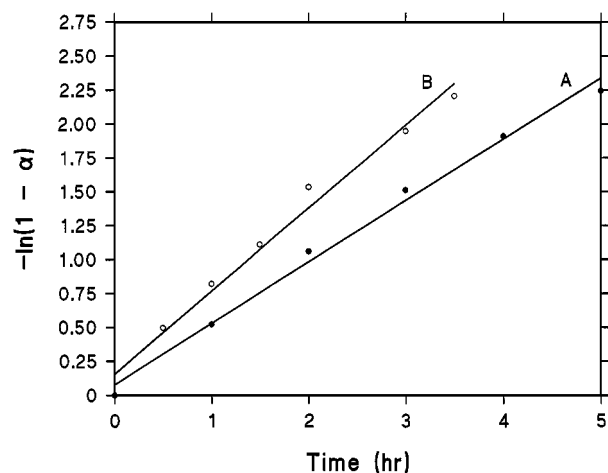


Figure 3  $-\ln(1 - \alpha)$  as a function of time in the system PBDI/UP in  $\text{CHCl}_3$  at  $60^\circ\text{C}$ ; uncatalyzed reaction (curve A), catalysed reaction (curve B).

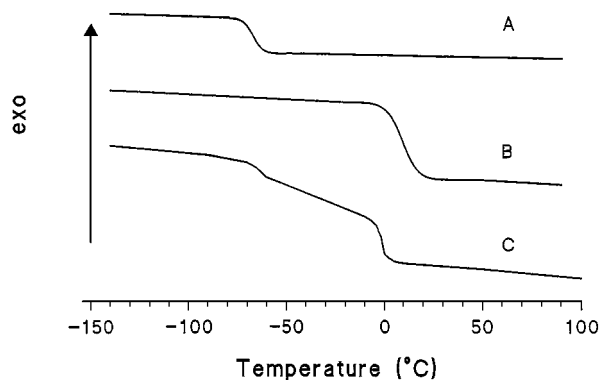


Figure 4 DSC thermograms of PBD (curve A), UP (curve B) and copolymer (curve C).

copolymer (curve C). The PBD rubber and UP resin show a glass transition temperature,  $T_g$ , at  $-71$  and  $8.5^\circ\text{C}$ , respectively. The thermogram of the copolymer shows two glass transitions at  $-66.5$  and  $-5.5^\circ\text{C}$ . The presence of two  $T_g$ s indicates that two distinct phases exist in the three-block copolymer.

Moreover, the  $T_g$  relative to the UP block is shifted at a lower value, while the  $T_g$  of the PBD block is detected at a higher value with respect to those of the pure components. These features confirm the formation of a block copolymer.

### 3.2. Spectroscopic and dynamic-mechanical analysis of the cured materials

The neat polyester resin and the blends prepared were investigated by transmission FT-IR spectroscopy in the form of finely ground powders, by using the KBr pellets technique.

The spectra of the plain UP resin before and after the curing process are reported in Fig. 5, while Fig. 6 shows the spectra relative to the UP/PBD 85/15 composition. The peaks characteristic of the double bonds of the styrene monomer and of the fumaric unsaturations

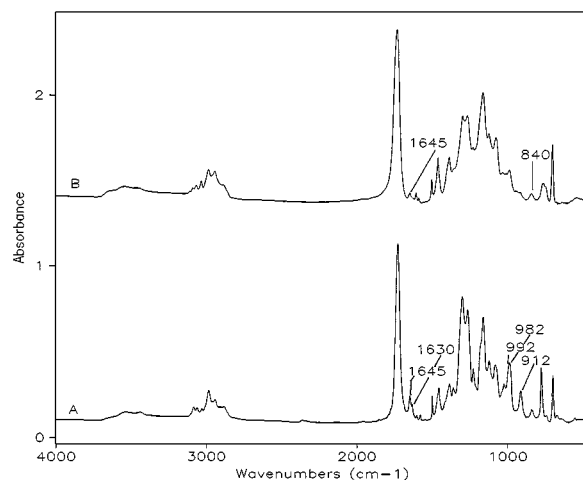


Figure 5 Transmission FT-IR spectra of uncured UP (curve A) and cured UP (curve B). Spectrum A was obtained on a thin film, and spectrum B on a KBr pellet.

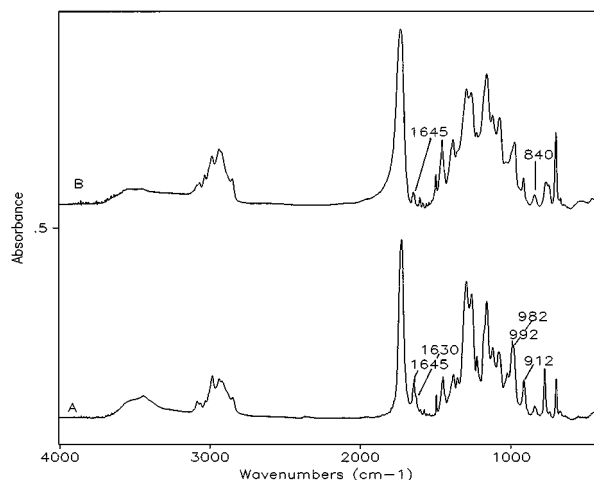


Figure 6 Transmission FT-IR spectra of the uncured (curve A) and cured (curve B) UP/PBD 85/15 blend. Spectrum A was obtained on a thin film, and spectrum B on a KBr pellet.

along the polyester backbone are clearly identified in the spectra of the uncured materials (see Figs 5 and 6, curves A). In particular, the styrene double bonds give rise to a  $\text{C}=\text{C}$  stretching at  $1630\text{ cm}^{-1}$ , a *trans*  $\text{HC}=\text{CH}$  wagging at  $992\text{ cm}^{-1}$  and a vinyl  $=\text{CH}_2$  wagging at  $912\text{ cm}^{-1}$ . The fumarate absorptions are located at  $1645\text{ cm}^{-1}$  ( $\text{C}=\text{C}$  stretching) and at  $840\text{ cm}^{-1}$  (*trans*  $\text{HC}=\text{CH}$  wagging). In the spectra of the cured materials (see Figs 5 and 6, curves B) the peaks of the styrene unsaturations are absent, thus indicating full conversion of the styrene monomer both in the plain resin and in the investigated blends. On the other hand, the fumarate peaks remain well detectable, which indicates that a fraction of double bonds along the polyester chains remain unreacted after the curing process.

The spectral data of Figs 5 and 6 allow one to estimate quantitatively the extent of residual unsaturations,  $R$ . This parameter can be expressed as

$$R = \frac{\bar{A}_{1645}}{\bar{A}_{1645}^0} 100 \quad (14)$$

where  $\bar{A}_{1645}$  is the ratio  $A_{1645}/A_{840}$  in the powder spectrum of the sample and  $\bar{A}_{1645}^0$  is the same absorbance ratio calculated for a thin film of the reactive mixture prior to the curing process. The peak at  $840\text{ cm}^{-1}$  is invariant with cure and is used for thickness normalization. The  $R$  values relative to the various investigated materials are reported in Fig. 7. The neat UP resin shows a residual unsaturation content of 25%, in good agreement with literature results [10]. In the binary blends, the  $R$  values are very close to that of the reference material, while in the ternary blends a slight increase of  $R$  is observed, up to a maximum value of 33% for the composition 85/15/3. Thus the rubber component alone does not influence the curing process of the matrix, while the presence of the emulsifying agent slightly reduces the final cross-link density of the UP resin.

In all the cases, however, the final conversion of the reactive groups, and hence the cross-link density achieved, remains high. This confirms that, even for the formulations highly doped with the rubber and the

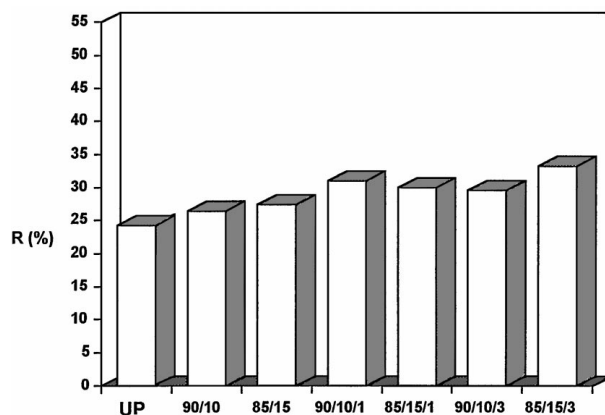


Figure 7 Residual fumaric unsaturations,  $R$ , for the net UP resin and for some binary and ternary blends. Compositions as indicated.

emulsifier, it is possible to obtain materials in which the thermosetting matrix retains its desirable properties in terms of rigidity and dimensional stability.

The above conclusions are confirmed by the dynamic-mechanical measurements performed on the cured samples.

The  $\tan \delta$  versus temperature curves relative to the plain resin, the 85/15 binary blend and the 85/15/3 ternary blend are reported in Fig. 8, curves A, B and C, respectively. The UP shows a main relaxation peak, associated with the glass transition, at  $155^\circ\text{C}$ , and an unresolved shoulder centred around  $70^\circ\text{C}$ . This secondary transition has been attributed to the styrene units bridging the polyester chains [11] and/or to the relaxation of short-chain segments in the vicinity of residual fumaric unsaturations (network defects) [12].

The dynamic mechanical spectra of the binary and ternary blends show, in addition to the UP transitions, a well-defined relaxation at about  $-60^\circ\text{C}$ , associated with the glass transition of the PBD rubber. This indicates that after curing, the system is phase separated, as will be further confirmed in the paragraph on the morphological analysis.

In the ternary blend the rubber peak is slightly broadened, possibly reflecting the formation of an interface

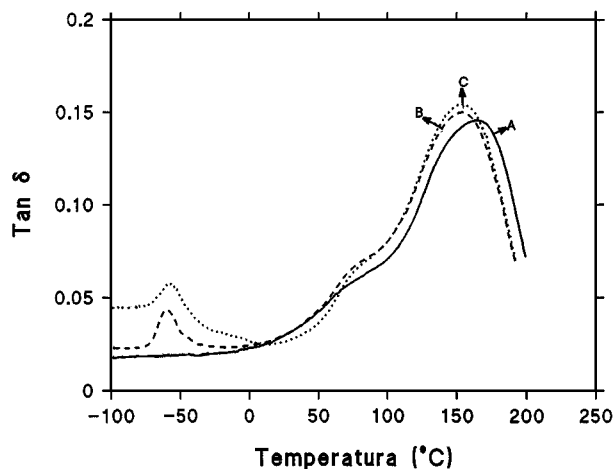


Figure 8 Dissipation factor,  $\tan \delta$ , as a function of the temperature for the UP (curve A), the UP/PBD 85/15 binary blend (curve B) and the UP/PBD/copolymer 85/15/3 ternary blend (curve C).

region due to the presence of the emulsifier. The main relaxation of the UP matrix in the blends shows a slight decrease towards lower temperatures with respect to the plain resin. Therefore it can be concluded, in agreement with the FT-IR analysis, that the addition of the rubber and the copolymer produce a very limited effect on the cross-linking density of the UP network.

### 3.3. Fracture properties and morphological analysis of the blends

Fracture mechanics tests, at low and high deformation rate, were performed on the various investigated blend systems, to evaluate the intrinsic toughness. At low deformation rate ( $1 \text{ mm min}^{-1}$ ), the fracture parameter,  $K_c$ , determined using Equation 1 is plotted as a function of blend composition in Fig. 9. It can be seen that, while in the case of the UP/PBD system (curve A), the  $K_c$  values remain practically unchanged with increasing the PBD content, for the UP/PBD/copolymer system (curves B, C and D) a substantial enhancement of toughness is found. In particular we observe that, for a given UP/PBD blend composition,  $K_c$  increases with increasing amount of copolymer. Similar results were obtained when the fracture data were expressed by the parameter  $G_c$ , Fig. 10. In terms of  $G_c$ , the addition of 5 parts by weight of copolymer to a blend containing 15 parts of rubber, leads to a  $G_c$  value which is about four times higher than that of the neat UP resin.

Fracture measurements were also performed under impact conditions ( $1 \text{ m s}^{-1}$ ) in order to evaluate the toughness of these materials under rapid loading. The corresponding  $K_c$  and  $G_c$  values are reported in Figs 11 and 12, respectively.

The behaviour of the impact toughness parameters is similar to that observed in the low-speed fracture tests, apart from a decrease in the absolute values of  $K_c$  and  $G_c$ . This effect is a direct consequence of the fact that, as the strain rate is enhanced, the capability of the material to be plastically deformed is strongly reduced.

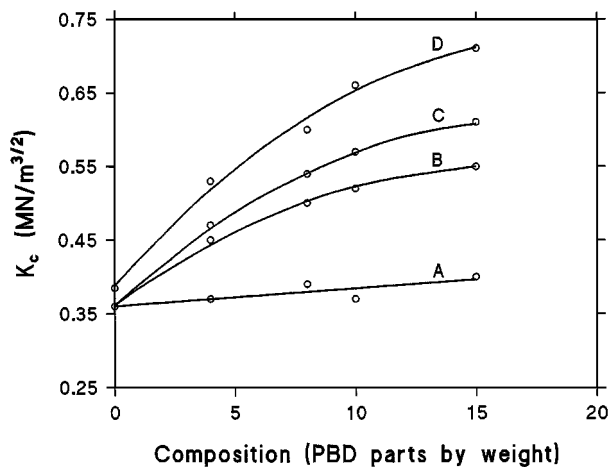


Figure 9 Critical stress intensity factor,  $K_c$ , as a function of the PBD content (parts by weight) for the UP/PBD binary blends (curve A) and for the UP/PBD/copolymer ternary blends. Curves B, C and D refer to the blends containing, respectively, 1, 3 and 5 parts by weight of the copolymer. Tests performed at low strain rate ( $1 \text{ mm min}^{-1}$ ).

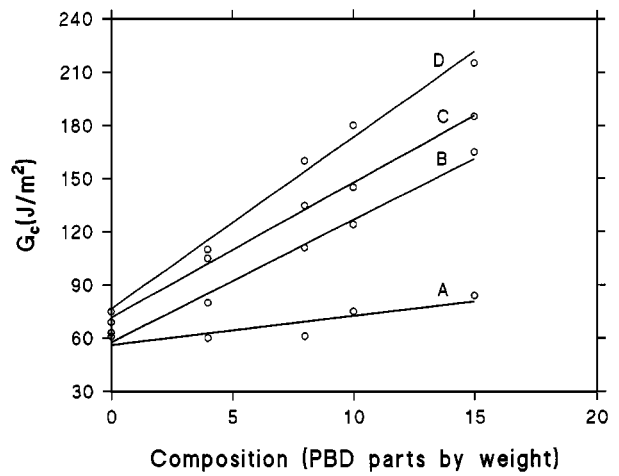


Figure 10 Critical strain energy release rate,  $G_c$ , as a function of the PBD content (parts by weight) for the UP/PBD binary blends (curve A) and for the UP/PBD/copolymer ternary blends. Curves B, C and D refer to the blends containing, respectively, 1, 3 and 5 parts by weight of the copolymer. Tests performed at low strain rate ( $1 \text{ mm min}^{-1}$ ).

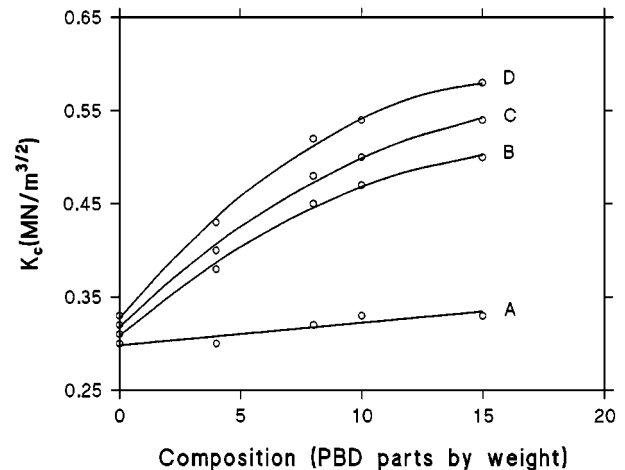


Figure 11 Critical stress intensity factor,  $K_c$ , as a function of the PBD content (parts by weight) for the UP/PBD binary blends (curve A) and for the UP/PBD/copolymer ternary blends. Curves B, C and D refer to the blends containing, respectively, 1, 3 and 5 parts by weight of the copolymer. Tests performed at high strain rate ( $1 \text{ m s}^{-1}$ ).

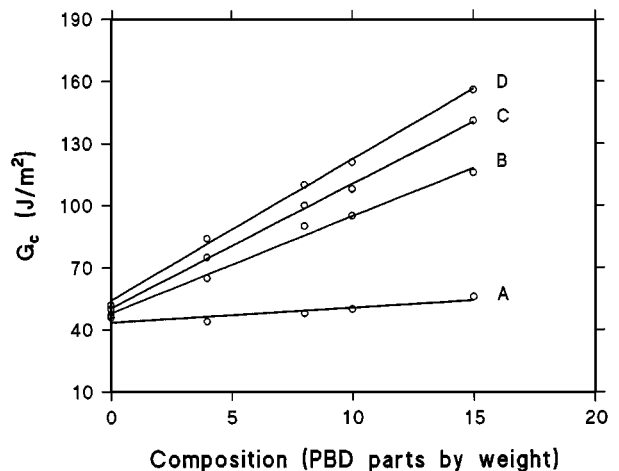


Figure 12 Critical strain energy release rate,  $G_c$ , as a function of the PBD content (parts by weight) for the UP/PBD binary blends (curve A) and for the UP/PBD/copolymer ternary blends. Curves B, C and D refer to the blends containing, respectively, 1, 3 and 5 parts by weight of the copolymer. Tests performed at high strain rate ( $1 \text{ m s}^{-1}$ ).

The whole of the fracture data clearly evince the role played by the copolymer as compatibilizing agent. In fact, one of the major effects of a compatibilizer is to increase the adhesion at phase boundaries, giving improved stress transfer within the material. Thus, for the UP/PBD/copolymer system, a good adhesion is realized so that the rubbery domains are able to act as load-bearing components favouring the initiation and the growth of shear-yielding deformations in the matrix. This mechanism, which is believed to be the main source of energy dissipation in multicomponent thermosetting systems [13–15], is scarcely operative in the case of the UP/PBD blends owing to a poor or no adhesion at the particle/matrix interface.

Further details on the effect of the copolymer occurring in these investigated blend systems were obtained by the morphological analysis performed on the surfaces of samples fractured at low deformation rate.

Fig. 13 shows scanning electron micrographs of UP/PBD blends containing 10 parts by weight of rubber. This micrograph reveals that the rubber is segregated into very large and inhomogeneous domains with diameters ranging from 30–100  $\mu\text{m}$ . Moreover, the UP matrix around the particles appears rather flat indicating the occurrence of a very limited plastic deformation, in accordance with the observed lack of toughness. The other UP/PBD blend compositions investigated display analogous fractographic features. When the copolymer is added to these binary UP/PBD blends, marked variations in the overall fracture morphology are clearly visible. In particular, as reported in Fig. 14, with increasing copolymer content the following features are observed:

- (i) a more homogeneous distribution of the rubbery domains within the UP matrix;
- (ii) a stronger decrease of the rubber particles dimensions. For example, in the case of a blend containing 10 parts by weight of PBD and 5 parts by weight of copolymer the domains size of the dispersed phase is reduced of about one order of magnitude with respect to the corresponding binary blend (compare Fig. 13 with Fig. 14c);

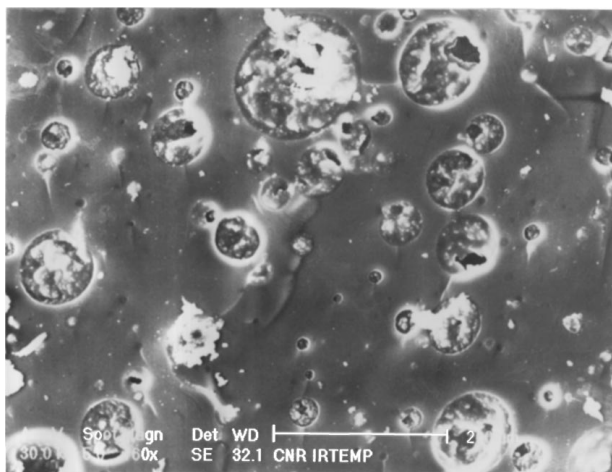
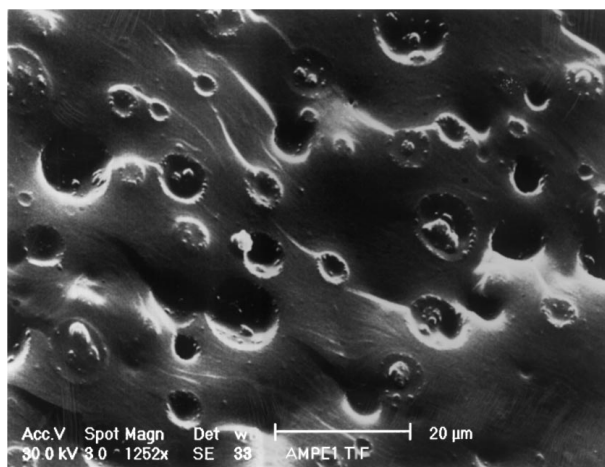
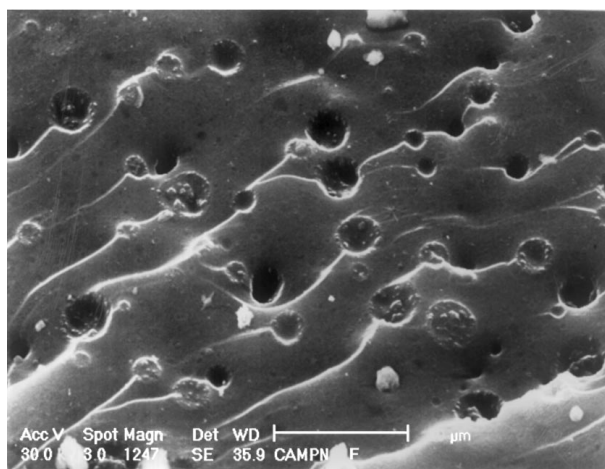


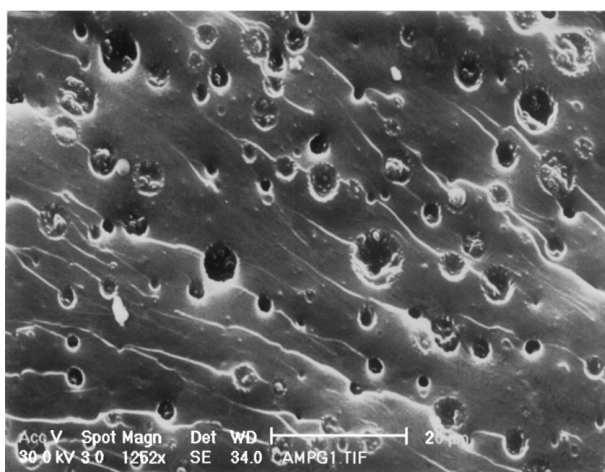
Figure 13 Scanning electron micrographs of the fracture surface of a binary UP/PBD blend. Composition 90/10 (parts by weight). Sample fractured at low strain rate ( $1 \text{ mm min}^{-1}$ ).



(a)



(b)



(c)

Figure 14 Scanning electron micrographs of the fracture surfaces of ternary blends: (a) UP/PBD/copolymer 90/10/1 (parts by weight); (b) UP/PBD/copolymer 90/10/3 (parts by weight); (c) 90/10/5 (parts by weight). Samples fractured at low strain rate ( $1 \text{ mm min}^{-1}$ ).

- (iii) a better adhesion at phase boundaries;
- (iv) an increase of localized shear yielding within the UP matrix and around the rubber particles.

All these aspects are due to the beneficial activity in the blends of the block copolymer which locates preferentially at the blend interfaces to reduce the interfacial

energy and promote a finer dispersion of one phase in other with improved interfacial adhesion. Therefore, the substantial improvement in toughness observed in the UP/PBD/copolymer system, can be ascribed to the particular type of morphology of the dispersed phase developed during the curing process. These structural features of the rubbery particles allow them to act as effective sites for the initiation and termination of multiple localized plastic deformations in the surrounding UP matrix. The formation of shear-bands which initiate at one particle and terminate at another are well visible in all the micrographs of these blend systems and occur to a greater extent as the copolymer content is enhanced. This type of mechanism, as already mentioned, is completely absent in the case of the UP/PBD blends mainly because of the weak adhesion at the interface which does not permit to the rubbery particles to act as crack arresters and hence to prevent premature fractures.

#### 4. Conclusion

A block copolymer was synthesized and used as compatibilizing agent for unsaturated polyester/rubber blends.

For the preparation of the copolymer, the hydroxyl-terminated groups of a polybutadiene rubber (PBD) were transformed into isocyanate groups (PBDI). The modified PBDI rubber was then reacted with a stoichiometric amount of UP resin. FT-IR spectroscopy showed that the isocyanate groups reacted quantitatively with the OH-end groups of the UP resin, forming a tri-block copolymer of the type UP-PBD-UP. The kinetics of this process was monitored via FT-IR spectroscopy.

Spectroscopic analysis of the cured samples demonstrated that, for all the investigated compositions, the final conversion of the reactive groups, and hence the cross-link density achieved, remains close to that of the plain UP resin.

Dynamic-mechanical measurements showed that the blends are phase separated, and further confirmed that the addition of the rubber and the copolymer produce a very limited effect on the cross-linking density of the UP network.

Fracture mechanics tests performed at high and low strain rate on the cured materials demonstrated a marked improvement in the fracture toughness parameters  $K_c$  and  $G_c$  when the copolymer was present. In particular, it was found that, for a given UP/PBD blend composition, the fracture toughness increased by

enhancing the copolymer content. These results were interpreted in terms of a morphological analysis performed on the fractured surfaces by SEM. The analysis showed increasing the amount of copolymer produced a finer and more homogeneous distribution of the particle size together with an improved adhesion at the phase boundary. This type of morphology allowed the rubber particles to act as effective controllers for the initiation and termination of extensive but localized shear-yielding deformations in the UP matrix.

The outlined mechanism, which was demonstrated to be the primary source of energy dissipation in the UP/PBD/copolymer blends, was completely absent in the case of the UP/PBD system.

#### Acknowledgements

The authors thank Professor G. Maglio for helpful and stimulating discussion of the results, and Mr V. Di Liello and Mr A. Lahoz for technical assistance.

#### References

1. M. MARGOLIS, "Advanced Thermoset Composites" (Van Nostrand Reinhold, New York, 1986).
2. P. EDELMAN and E. McMAHON, *Compos. Technol. Rev.* **1**(2) (1979) 7.
3. BURNS, "Polyester Molding Compound" (Marcel Dekker, New York, 1982).
4. S. NEWMAN and D. FESKO, *Polym. Compos.* **5** (1) (1984) 88.
5. E. MARTUSCELLI, P. MUSTO, G. RAGOSTA, G. SCARINZI and E. BERTOTTI, *J. Polym. Sci. B Polym. Phys. Ed.* **31** (1993) 619.
6. M. ABBATE, E. MARTUSCELLI, P. MUSTO, G. RAGOSTA and M. LEONARDI, *J. Appl. Polym. Sci.* **62** (1996) 2107.
7. WILLIAMS, "Fracture Mechanics of Polymers" (Wiley, New York, 1984).
8. W. F. BROWN and J. SRAWLEY, ASTM STP4 (American Society for Testing and Materials, Philadelphia, PA, 1966) p. 13.
9. E. PLATI and J. G. WILLIAMS, *Polym. Eng. Sci.* **15** (1975) 470.
10. E. MARTUSCELLI, P. MUSTO, G. RAGOSTA and G. SCARINZI, *Polymer* **37** (1996) 4025.
11. R. S. LENK and J. C. PADGET, *Eur. Polym. J.* **11** (1975) 327.
12. D. MELOT, B. ESCAIG, J. M. LEFEBRE, R. P. EUSTACHE and F. LAUPRETE, *J. Polym. Sci. Polym. Phys.* **32** (1994) 249.
13. A. J. KINLOCK and J. YOUNG, "Fracture Behaviour of Polymers" (Applied Sciences, London, 1983).
14. R. A. PEARSON and A. F. YEE, *J. Mater. Sci.* **21** (1986) 2475.
15. W. D. BACOM, R. L. COTTING, R. L. JONES and P. PEYSER, *J. Appl. Polym. Sci.* **19** (1975) 2545.

Received 31 October 1997  
and accepted 27 July 1998